

Deficiency in the 15-kDa Selenoprotein Inhibits Tumorigenicity and Metastasis of Colon Cancer Cells

Robert Irons^{1,3,4}, Petra A. Tsuji^{1,2,3}, Bradley A. Carlson³, Ping Ouyang^{1,3}, Min-Hyuk Yoo³, Xue-Ming Xu³, Dolph L. Hatfield³, Vadim N. Gladyshev⁵, and Cindy D. Davis¹

Abstract

Selenium has cancer-preventive activity that is mediated, in part, through selenoproteins. The role of the 15-kDa selenoprotein (Sep15) in colon cancer was assessed by preparing and using mouse colon CT26 cells stably transfected with short hairpin RNA constructs targeting Sep15. Metabolic ⁷⁵Se labeling and Northern and Western blot analyses revealed that >90% of Sep15 was downregulated. Growth of the resulting Sep15-deficient CT26 cells was reduced ($P < 0.01$), and cells formed significantly ($P < 0.001$) fewer colonies in soft agar compared with control CT26 cells. Whereas most (14 of 15) BALB/c mice injected with control cells developed tumors, few (3 of 30) mice injected with Sep15-deficient cells developed tumors ($P < 0.0001$). The ability to form pulmonary metastases had similar results. Mice injected with the plasmid-transfected control cells had >250 lung metastases per mouse; however, mice injected with cells with downregulation of Sep15 only had 7.8 ± 5.4 metastases. To investigate molecular targets affected by Sep15 status, gene expression patterns between control and knockdown CT26 cells were compared. Ingenuity Pathways Analysis was used to analyze the 1,045 genes that were significantly ($P < 0.001$) affected by Sep15 deficiency. The highest-scored biological functions were cancer and cellular growth and proliferation. Consistent with these observations, subsequent analyses revealed a G₂-M cell cycle arrest in cells with targeted downregulation of Sep15. In contrast to CT26 cells, Sep15-targeted downregulation in Lewis lung carcinoma (LLC1) cells did not affect anchorage-dependent or anchorage-independent cell growth. These data suggest tissue specificity in the cancer-protective effects of Sep15 downregulation, which are mediated, at least in part, by influencing the cell cycle. *Cancer Prev Res*; 3(5); 630–9. ©2010 AACR.

Introduction

Colorectal cancer is the third most commonly diagnosed cancer in Americans and is the second leading cause of cancer mortality. Epidemiologic, clinical, and preclinical studies provide evidence that the essential trace mineral selenium may protect against colon cancer (1). Supplemental selenium has been found to reduce the incidence and mortality of colon cancer in humans (2). This is consistent with animal studies showing protective effects of selenium

against carcinogen-induced aberrant crypt formation and colon tumor development (3, 4). Some of these biological changes are likely attributable to the role of selenium as a constituent of specific proteins. Moreover, recent studies have implicated both selenoproteins and low molecular weight selenocompounds as playing important roles in the cancer-protective effects of selenium in the colon (5).

The 15-kDa selenoprotein gene (*Sep15*) is one of 24 known selenoprotein genes in rodents (6). The gene product, Sep15, exhibits redox activity (7) and belongs to the class of thiol-disulfide oxidoreductase-like selenoproteins (8). Sep15 is structurally similar to the thioredoxin superfamily (8). Although decreased expression of Sep15 has been observed in liver, prostate, and lung cancer, the expression of Sep15 in colon cancer is less clear (7). Analysis of the National Cancer Institute's Developmental Therapeutics Program database (<http://dtp.nci.nih.gov/mtweb/targetdata>), which screens 60 tumor cell lines for molecular targets, showed increased Sep15 expression in colon cancer cell lines compared with other cancers as well compared with other selenoproteins. Moreover, in humans, *Sep15* is located on chromosome 1p31, a locus commonly mutated in human cancer (9).

The purpose of this study was to assess the role of Sep15 in colon cancer. RNA interference technology was used to

Authors' Affiliations: ¹Nutritional Science Research Group and ²Cancer Prevention Fellowship Program, National Cancer Institute, Rockville, Maryland; ³Molecular Biology of Selenium Section, Laboratory of Cancer Prevention, National Cancer Institute, Bethesda, Maryland; ⁴V.E. Irons, Inc., Kansas City, Missouri; and ⁵Brigham and Women's Hospital, Harvard Medical School, Boston, Massachusetts

Note: Supplementary data for this article are available at Cancer Prevention Research Online (<http://cancerprevres.aacrjournals.org/>).

R. Irons and P.A. Tsuji are co-first authors.

Corresponding Author: Cindy D. Davis, Nutritional Science Research Group, Division of Cancer Prevention, National Cancer Institute, 6130 Executive Boulevard, Suite 3159, Rockville, MD 20892-7328. Phone: 301-594-9692; Fax: 301-480-3925; E-mail: davisci@mail.nih.gov.

doi: 10.1158/1940-6207.CAPR-10-0003

©2010 American Association for Cancer Research.

specifically downregulate Sep15 expression in a mouse colon cancer cell line, CT26. These cells were derived from an *N*-nitroso-*N*-methylurethane-induced BALB/c undifferentiated colon carcinoma (10). Herein, we report that targeted downregulation of Sep15 in CT26 cells decreased growth under anchorage-dependent and anchorage-independent conditions, inhibited tumor formation *in vivo*, and reduced lung metastasis. In contrast, targeted downregulation of Sep15 in mouse Lewis lung carcinoma (LLC1) cells did not affect the ability of the cells to grow in culture or in soft agar. These studies reveal a complex role of Sep15 in cancer development.

Materials and Methods

The murine CT26 colon cancer and LLC1 lung cancer cells were purchased from the American Type Culture Collection. ^{75}Se (specific activity, $\sim 1,000$ Ci/mmol) was obtained from the Research Reactor Facility at the University of Missouri (Columbia, MO), and $[\alpha\text{-}^{32}\text{P}]\text{dCTP}$ (specific activity, $\sim 6,000$ Ci/mmol) was from Perkin-Elmer. pSilencer 2.0 U6 Hygro vector was purchased from Ambion, and Hybond N^+ nylon membranes were from GE Healthcare. RPMI 1640, fetal bovine serum, hygromycin B, NuPAGE 4% to 12% polyacrylamide gels, lithium dodecyl sulfate sample buffer, SeeBlue Plus2 protein markers, polyvinylidene difluoride membranes, Lipofectamine 2000, and Trizol reagent were purchased from Invitrogen, and 5,5'-dithiobis(2-nitrobenzoic acid) and aurothioglucose were from Sigma-Aldrich.

Antibodies against Sep15 were generated in our laboratories using recombinant Sep15 as antigen. Horseradish peroxidase-conjugated secondary antibody was obtained from Santa Cruz Biotechnology, and SuperSignal West Dura substrate was from Pierce. iScript cDNA Synthesis kit and SYBR Green Supermix were purchased from Bio-Rad Laboratories. Primers for real-time PCR were purchased from Sigma-Genosys, noble agar was from Becton Dickinson, and black India ink was from Winsor & Newton. Other reagents used were commercially available and were of the highest quality available.

Targeted downregulation of Sep15

The pU6-m3 vector used for generating short hairpin RNA (shRNA) targets was constructed as described elsewhere (11, 12). To downregulate *Sep15* expression, two separate 19-nucleotide sequences, 5'-gcaccacagtcataat-3' (shSep15-1) and 5'-acagaagagttccattaa-3' (shSep15-2), were chosen from the mouse *Sep15* cDNA, which were unique to this gene. These sequences were annealed and inserted into the *Bam*HI-*Hind*III cloning sites in pU6-m3 as previously described (11).

Culture of mammalian cells and cell growth assays

CT26 cells were cultured in growth medium (RPMI 1640 supplemented with 10% fetal bovine serum, 1% sodium pyruvate, and 500 $\mu\text{g}/\text{mL}$ hygromycin B) in a humidified atmosphere with 5% CO_2 at 37°C. LLC1

cells were cultured in DMEM (supplemented with 10% heat-inactivated fetal bovine serum and 500 $\mu\text{g}/\text{mL}$ hygromycin B). Both malignant cell lines were stably transfected with shSep15-1, shSep15-2, or pU6-m3 constructs using Lipofectamine 2000 by selecting cells in the presence of 500 $\mu\text{g}/\text{mL}$ hygromycin B.

Cell growth was monitored by seeding cells in six-well plates at 1×10^5 per well in complete growth medium and counting cells for 4 d. For the cell growth assays under conditions of varying selenium concentrations, CT26 cells were seeded in six-well plates at 2×10^5 per well in complete culture medium, wherein the cells attached to the bottom of the wells. After 24 h, growth medium was discarded, and cells were washed twice with PBS and subsequently fed with 2 mL of serum-free medium (RPMI 1640 supplemented with 1% sodium pyruvate, 500 $\mu\text{g}/\text{mL}$ hygromycin B, 5 $\mu\text{g}/\text{mL}$ insulin, and 5 $\mu\text{g}/\text{mL}$ transferrin) supplemented with none, 0.1 $\mu\text{mol}/\text{L}$, 0.5 $\mu\text{mol}/\text{L}$, or 1.0 $\mu\text{mol}/\text{L}$ selenium in the form of sodium selenite. The total number of cells was counted daily for 4 d in serum-free medium.

Real-time reverse transcription-PCR analysis

Total RNA was extracted from cells using Trizol reagent. cDNA was synthesized using iScript with 2 μg of total RNA. For real-time quantitative PCR, 1.5 μL cDNA was used in 20 μL reactions using the DNA Engine Opticon 2 Real-Time PCR Detection System (MJ Research/Bio-Rad Laboratories). The primers used for real-time PCR are shown in Supplementary Table S1. The mRNA levels of selenoproteins were calculated relative to the expression of β -glucuronidase (*Gusb*), and/or glyceraldehyde-3-phosphate dehydrogenase (GAPDH) was used as the internal control.

Western blot analysis

Protein extracted from the three CT26 cell lines was electrophoresed on a NuPAGE 4% to 12% polyacrylamide gel followed by transferring to a polyvinylidene difluoride membrane. The membrane was incubated with a rabbit polyclonal Sep15 antibody overnight. Horseradish peroxidase-conjugated anti-rabbit secondary antibody (1:5,000) was applied, and the membrane was incubated in chemiluminescent substrate and exposed to X-ray film.

^{75}Se -labeling of cells

CT26 cells were seeded in a six-well plate (5×10^5 per well), incubated for 18 hours, and then labeled with 50 $\mu\text{Ci}/\text{well}$ of ^{75}Se for 24 hours before harvesting. Cells were suspended in 1 \times NuPAGE lithium dodecyl sulfate sample buffer and sonicated, and 20 μg protein was electrophoresed on a NuPAGE 4% to 12% polyacrylamide gel. The gel was stained with Coomassie blue, dried, and exposed to a PhosphorImager screen (Molecular Dynamics, GE Healthcare).

Northern blot analysis

Total RNA was isolated using Trizol reagent. An equal amount of RNA (15 μg) from each cell line was loaded

onto gels and transferred to a nylon membrane. The membrane was hybridized with a ^{32}P -labeled Sep15 cDNA probe prepared as described previously (13). The membrane was stripped and reprobed with a ^{32}P -labeled GAPDH cDNA probe.

Enzyme activities

Glutathione peroxidase (GPx) activity was measured by the coupled assay procedure (14), which uses hydrogen peroxide as substrate. This assay measures both GPx1 and GPx2 activity. Data are expressed as units/mg protein. TR activity was determined spectrophotometrically by the method of Holmgren and Björnstedt (15) as modified by Hill et al. (16) and Hintze et al. (17). Activity was determined by subtracting the time-dependent increase in absorbance at 412 nm in the presence of the thioredoxin reductase activity inhibitor aurothioglucose from total activity. A unit of activity was defined as 1.0 μmol 5-thio-2-nitrobenzoic acid formed/min/mg protein. Protein concentrations were measured using the bicinchoninic acid reagent.

Soft agar assay

Anchorage-independent growth was assayed as described previously (11) with the exception that herein a total of 3,000 cells of each stably transfected CT26 cell line were suspended in 3 mL of 0.35% agar in complete RPMI 1640 and spread onto 60-mm Petri dishes masked with a basal layer of 3 mL of 0.7% agar in medium. For LLC1 cells, a total of 1,000 cells/3 mL were applied. Cells were incubated at 37°C for 20 d (12 d for LLC1 cells), and complete growth medium was applied to the dishes every 3 to 5 d. The colonies were visualized by staining with *p*-iodonitrotetrazolium violet overnight, scanned, and counted.

Cell cycle analysis

CT26 cells were grown in complete medium to 40% confluency, washed twice with PBS, and maintained in serum-free medium for 48 h to induce G_0 - G_1 cell cycle synchronization. Cells were then washed twice with PBS and growth stimulated with complete growth medium for 24 hours. Cells were then twice washed with PBS, trypsinized, and suspended in PBS (1×10^7 to 2×10^7 cells/mL) on ice. Ice-cold 70% ethanol was added gradually, and cells were fixed overnight. Cells were centrifuged and re-suspended in RNase (100 units) and incubated at 37°C for 20 minutes. The suspension was stained with propidium iodide in the dark at 4°C overnight, filtered through a 50- μm mesh, and acquired with a FACSCalibur (Becton Dickinson). The number of cells in each phase of the cell cycle was analyzed by ModFit LT version 3.0 (Verity).

Microarray analysis

mRNA was isolated from plasmid-transfected control and shSep15 knockdown CT26 cells ($n = 3$ for each). Microarray analysis was done on Affymetrix Mouse 430_2 gene chips. Three arrays were analyzed from different mRNA samples for each construct. The false discovery rate was set at <0.01 . Controls and cells with targeted

downregulation of Sep15 were compared by ANOVA. The ANOVA list can be calculated from our data accessible through Gene Expression Omnibus Series accession number GSE20390 (<http://www.ncbi.nlm.nih.gov/geo/query/acc.cgi?acc=GSE20390>). Those genes significantly different from the control cells at the $P < 0.001$ level were subjected to functional gene analysis using the DAVID functional annotation tool (18, 19) and the Ingenuity Pathway Analysis (IPA; version 7.5). IPA groups significantly linked genes according to the biological processes in which they function. The program displays their significance values, the interacting genes, and direct or indirect association patterns. The networks created were ranked depending on the number of significantly expressed genes they contain.

Animal studies

All animal protocols and animal care were in accordance with the NIH's guidelines for care and use of laboratory animals under the direction of Dr. John Dennis (National Cancer Institute, NIH, Bethesda, MD). Male BALB/c mice were obtained from The Jackson Laboratory and maintained in a temperature- and humidity-controlled animal facility with a 12-h light/dark cycle. Animals were given free access to water and were monitored closely for any clinical signs of poor health throughout the study.

Three-week-old male BALB/c mice were maintained on a selenium-deficient Torula yeast-based diet that was supplemented with 0, 0.1, or 2.0 μg selenium/g diet as sodium selenite (Teklad, Harlan Laboratories) for 3 weeks before being injected s.c. with 1×10^6 CT26 cells ($n = 5$ for plasmid-transfected controls, shSep15-1 cells, or shSep15-2 cells on each diet) in 200 μL PBS. Animals were sacrificed 3 wk after injection. Tumors, if present, were excised, measured, weighed, and snap frozen and stored at -80°C for future analyses.

For the lung metastasis study, 6-wk-old male BALB/c mice were maintained on mouse chow for 3 wk before i.v. injection into the tail vein with plasmid-transfected control or shSep15 CT26 cells (5×10^5 per mouse) in 200 μL PBS. Animals were sacrificed and lungs were examined 12 days after i.v. injection. Three milliliters of 15% India ink/PBS solution were injected into the lungs through the trachea. Lung tissues were excised and "bleached" by Fekete's solution (60% ethanol, 3.2% formaldehyde, and 0.75 mol/L acetic acid). Lobes of the lungs were separated and the pulmonary metastatic lesions formed on the surface of each lung were counted under a dissecting microscope. Lungs with >250 metastatic lesions were assigned a value of 250 because of the inherent difficulty to reliably count numbers over 250 lesions per lung. Three independent experiments were conducted.

Statistical analyses

Data are presented as the mean \pm SE. Data were analyzed by ANOVA followed by Tukey's multiple comparison post hoc test using GraphPad Prism (version 4). The level of significance was set at $P < 0.05$.

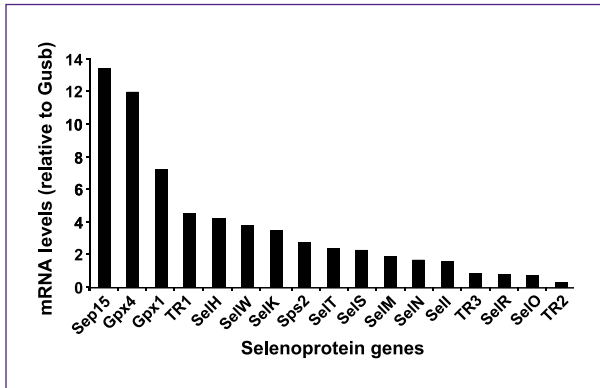


Fig. 1. Selenoprotein mRNA expression in CT26 cells. Cells were grown, RNA was extracted, and mRNA levels for indicated selenoproteins were determined by RT-PCR analysis as described in Materials and Methods. *Gusb* was used as the internal control.

Results

Gene expression for all 24 mouse selenoprotein genes was determined in CT26 cells by real-time PCR analysis (Fig. 1). Seventeen selenoprotein mRNAs were detected. Sep15 mRNA had the highest mRNA expression level, and other highly expressed genes included GPx4 and GPx1. To prepare cells characterized by Sep15 deficiency, CT26 cells were stably transfected with shSep15-1, shSep15-2, or the corresponding pU6-m3 control constructs. Each of the stably transfected cell lines was initially labeled with ^{75}Se to examine the levels of Sep15 and other selenoproteins, and the relative intensities of ^{75}Se -labeled proteins were determined using a PhosphorImager (Fig. 2A). Both cells with targeted downregulation of Sep15 significantly re-

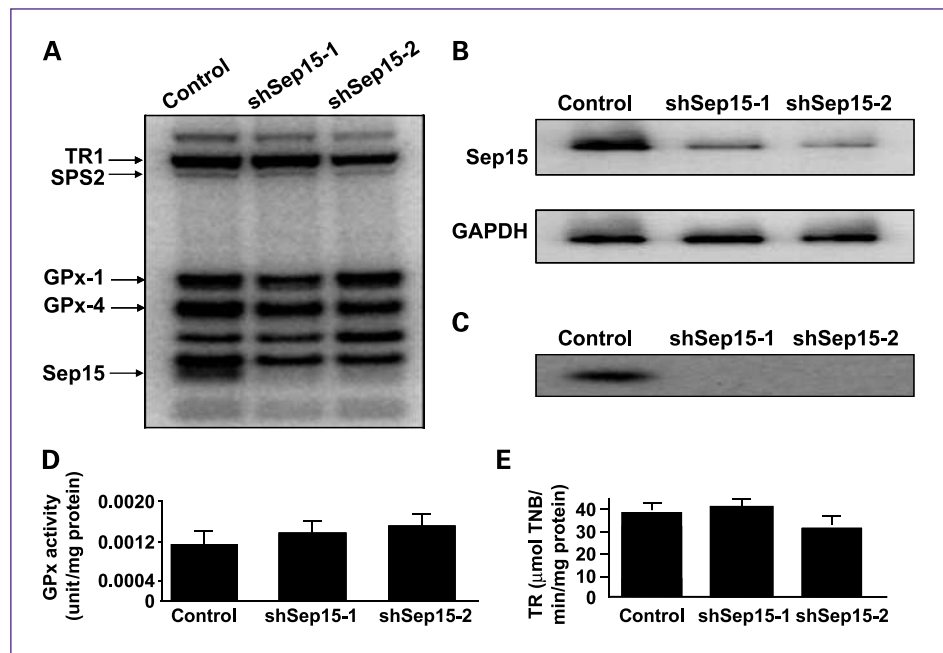
duced the levels of ^{75}Se -labeled Sep15. Northern (Fig. 2B) and Western (Fig. 2C) blot analyses also showed that Sep15 mRNA and protein expression, respectively, were efficiently (>90%) decreased by both shRNA vectors. In contrast, ^{75}Se labeling of other selenoproteins, such as TR1, GPx1, and GPx4, did not change (Fig. 2A) nor were their catalytic activities (Fig. 2D and E) affected by the shSep15 constructs.

The growth rate of the shSep15-1 and shSep15-2 mouse colon carcinoma CT26 cells was significantly reduced ($P < 0.01$) beginning at 3 days and was 40% to 50% fewer cells at 4 days compared with the pU6-m3-transfected control cells (Fig. 3A). Changing the selenium concentration in the growth medium from 0 to 1 $\mu\text{mol/L}$ did not significantly affect cell growth of the cells with Sep15-targeted downregulation compared with the control cells (Supplementary Fig. S1).

To extend these findings to other cell lines, stably transfected mouse LLC1 cells with the same constructs for Sep15-targeted downregulation as the CT26 cells were developed. A >90% knockdown efficiency was achieved as verified by real-time reverse transcription-PCR (RT-PCR; Supplementary Fig. S2A). Whereas the basal expression of Sep15 is higher in CT26 than in LLC1 cells (27.65 versus 5.31 units relative to *Gusb*, respectively), this level of expression is still ~10-fold higher than in the CT26 cells with targeted downregulation of Sep15 (0.59 unit relative to *Gusb*). However, in contrast to the growth of CT26 cells, the growth rate of shSep15-1-transfected and shSep15-2-transfected LLC1 cells was not altered compared with that of the pU6-m3-transfected LLC1 control cells (Supplementary Fig. S2B).

Another characteristic of many cancer cells is their ability to grow unanchored in soft agar, whereas many normal cells do not grow under such conditions. After 20 days of growth

Fig. 2. Targeted removal of Sep15 in CT26 cells. Cells were stably transfected with the pU6-m3 control, shSep15-1 construct, or shSep15-2 construct (as indicated), and the expression of Sep15 was examined by labeling cells with ^{75}Se (A), Northern blotting (B), or Western blotting (C). Transfected cells were also analyzed for GPx (D) and thioredoxin reductase (E) activities. Columns, mean ($n = 3$); bars, SE.



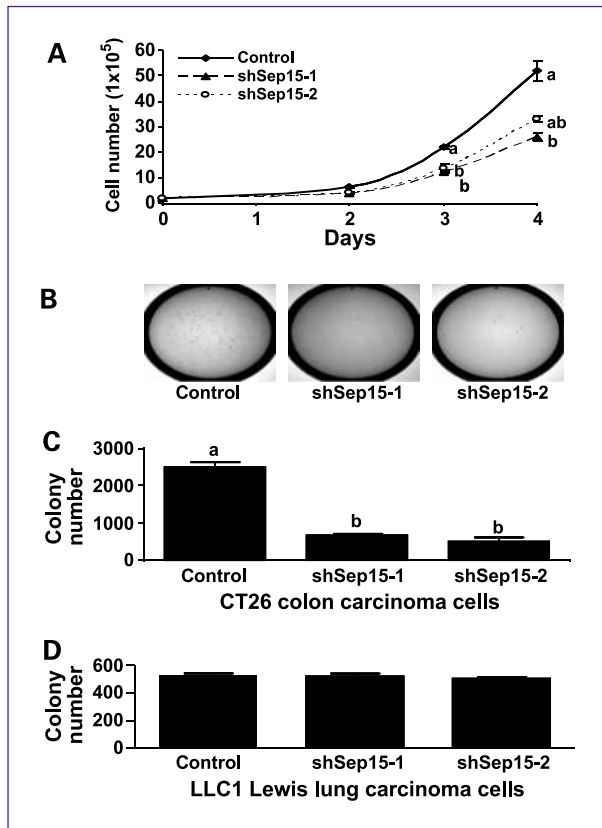


Fig. 3. Effects of targeted downregulation of Sep15 on cell growth and colony formation in soft agar in CT26 and LLC1 cells. A, growth rates of cells transfected with the pU6-m3 control, shSep15-1 construct, or shSep15-2 construct. Ability of cells transfected with the pU6-m3 control, shSep15-1 construct, or shSep15-2 construct to grow in soft agar. CT26 colonies were stained with *p*-iodonitrotetrazolium overnight (B) and the stained colonies were counted and recorded (C). D, the ability of LLC1 cells transfected with the control, shSep15-1, and shSep15-2 constructs to grow in soft agar was assessed and quantitated. Columns, mean ($n = 3$ for CT26 cells and $n = 8$ for LLC1 cells); bars, SE. Data are indicative of three independent experiments. Means not sharing a common letter are significantly different ($P < 0.01$).

in soft agar, the colonies of cells transfected with either the pU6-m3 control or the Sep15-targeted downregulation constructs were stained, scanned, and quantitated (Fig. 3B). Compared with the pU6-m3-transfected control cells, the shSep15-1-transfected and shSep15-2-transfected CT26 cells had formed significantly ($P < 0.01$) fewer colonies ($2,470 \pm 140$ versus 668 ± 33 and 512 ± 83 colonies, respectively; Fig. 3C). In contrast to the findings with CT26 colon carcinoma cells, Sep15-targeted downregulation in LLC1 lung carcinoma cells did not affect the ability of cells to grow in soft agar. The shSep15-1-transfected and shSep15-2-transfected cells formed 521 ± 19 and 505 ± 10 colonies, respectively, whereas the control LLC1 cells had 529 ± 12 colonies (Fig. 3D). These data suggest that Sep15-targeted downregulation in LLC1 cells does not influence anchorage-dependent or anchorage-independent cell growth.

The ability of CT26 cells with targeted downregulation and control cells to form tumors was measured by injecting them s.c. into mice of the same genetic background. Control cells retained their tumorigenic ability and resulted in subcutaneous tumors in injected mice (Fig. 4A). Most (14 of 15) of the animals injected with control cells developed tumors; dietary selenium seemed to dose dependently decrease tumor weight in animals injected with control cells. In contrast, only 1 of 15 of the animals injected with shSep15-2 CT26 cells developed a tumor ($P < 0.0001$). Moreover, because the constructs were retained in stably transfected cells with hygromycin B, and the injected mice could not be treated with this antibiotic, it was possible that the tumor that grew in the mouse injected with shSep15-2-transfected cells was a result of loss of the shSep15 targeting vector. Indeed, RT-PCR analysis showed that tumors from both the control and cells with targeted downregulation expressed appreciable Sep15 mRNA (Fig. 4B). However, because only one tumor was formed when the shSep15-2 knockdown cells were used, another 15 mice with the shSep15-1 knockdown cells were examined. Similar to the results with the shSep15-2 knockdown cells, very few animals injected with shSep15-1 were able to develop tumors (2 of 15), and the tumors that were formed had no difference in Sep15 expression compared with tumors formed in mice injected with control cells (0.13 ± 0.02 units versus 0.18 ± 0.07 units relative to GAPDH; $P > 0.05$). These data suggest that residual tumor growth in mice injected with the shSep15-transfected cells is dependent on Sep15 expression.

In addition to inhibiting tumor growth, targeted downregulation of Sep15 also inhibited the ability to form pulmonary metastatic lesions on i.v. administration of cells (Fig. 4C and D). Mice injected with the plasmid-transfected control cells had >250 lung metastases per mouse; however, mice injected with the shSep15 cells only had 8 ± 5 metastases.

Microarray analysis was conducted to elucidate possible mechanism(s) whereby Sep15 deficiency inhibited CT26 cancer cell growth, ability to grow in soft agar, tumorigenicity, and metastasis. Comparison of gene expression changes between cells with targeted downregulation of Sep15 and pU6-m3 control cells revealed 1,045 of a total number of 45,101 genes and their variants examined that were statistically ($P < 0.001$ level) different. The most significantly upregulated and downregulated genes and their protein products are listed in Table 1. Further examination with the DAVID functional annotation gene ontology tool showed that genes in several areas were affected, including cell cycle (G_2 -M-phase arrest), protein localization, and metabolism. Analysis with IPA showed that the top 5 associated networks were related to cancer, cell cycle, or cellular function and maintenance. These included "cellular assembly and organization/cellular function and maintenance/cell morphology," "DNA replication/recombination and repair/cell cycle/cancer," and "cancer/cell-to-cell signaling and interaction/cellular function and maintenance" (Fig. 5). Genes depicted in red have upregulated and genes

in green have downregulated expression in shSep15 knockdown cells compared with control cells. A list of the genes that had the most significantly increased or decreased expression in the Sep15-targeted downregulation compared with the control cells is shown in Table 1. The gene whose expression changed the most was *Ccnb1ip1*. When the significantly altered genes were analyzed for biological function, the primary disease being altered was cancer (302 significantly modified genes) and the primary molecular and cellular function was cellular growth and proliferation (246 significantly modified genes) and cell death (216 significantly modified genes).

Quantitative RT-PCR was used to validate the results of the microarray analysis. Comparison of data from quantitative RT-PCR and microarray showed a similar magnitude and direction of the response in the mRNA expression of cyclin B1-interacting protein 1 (CCNB1IP1; 10.03- and 13.52-fold increased expression via quantitative RT-PCR and microarray, respectively) and cyclin B1 (4.8- and 2.4-fold increased expression via quantitative RT-PCR and microarray, respectively) in cells with targeted downregulation compared with control cells. Similar results were also observed for several selenoprotein genes (*Sep15*, *GPx1*, *GPx4*, *SelM*, and *SelK*). For example, Sep15 was inhibited 98.2% and 95.3% when analyzed by quantitative RT-PCR and microarray, respectively. None of the other selenoproteins showed significant changes in gene expression.

Fluorescence-activated cell sorting (FACS) analysis was then used to validate the G₂-M cell arrest suggested by

the microarray analysis. The shSep15 cells had a higher percentage of cells in G₂-M (21.2 ± 1.1% versus 13.3 ± 0.9%) and G₀-G₁ (57.3 ± 1.4% versus 51.0 ± 1.1%) and a smaller percentage of cells in S phase (21.6 ± 0.5% versus 35.7 ± 0.5%, mean ± SE, *n* = 8) compared with the control cells.

Discussion

Whereas recent data have shown that both selenoproteins and low molecular weight selenocompounds may mediate the cancer-protective effects of selenium, few studies have addressed the role of specific selenoproteins (5). The current studies help with this void by evaluating selenoprotein expression in mouse CT26 colon cancer cells. Because Sep15 was the highest expressed selenoprotein mRNA in these cells and little is known about its biological effects, cells with targeted downregulation of Sep15 were then generated by stable transfection with two different Sep15-specific sequences and compared with plasmid-transfected control cells. Surprisingly, the cells with targeted downregulation of Sep15 exhibited decreased colony formation in soft agar (Fig. 3), as well as lower tumor formation and decreased ability to form lung metastasis (Fig. 4) compared with the control cells. Because the Sep15-deficient cell lines and the corresponding CT26 parental cells were transfected with identical vectors [described in detail elsewhere (11, 20–22)] except for the shRNAs in the two Sep15 downregulated cells, these changes are most certainly due to the loss of this selenoprotein. These results suggest that targeted

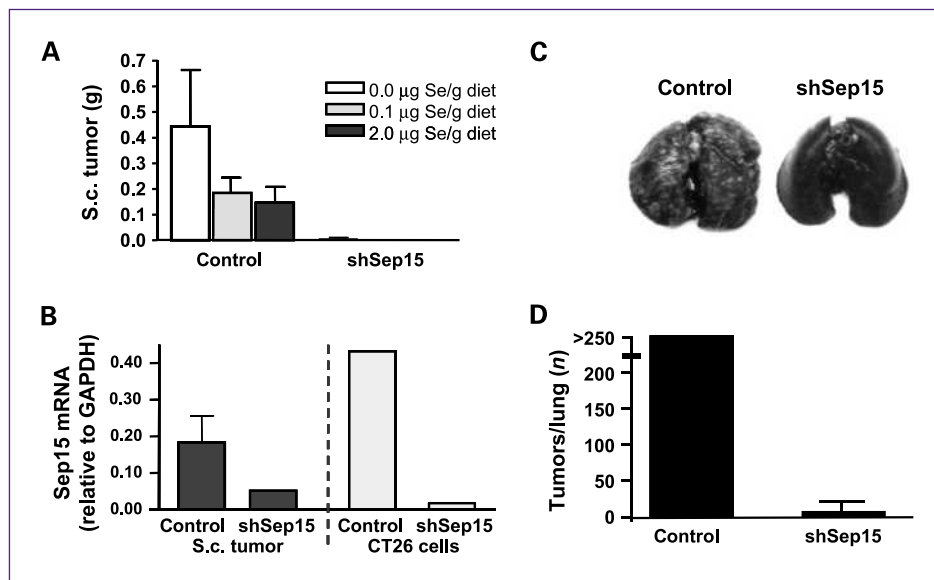


Fig. 4. Effects of targeted downregulation of Sep15 on primary tumor formation and lung metastases in BALB/c mice. A, mice maintained on Se-deficient (0 µg S/g), Se-sufficient (0.1 µg S/g), and Se-enriched (2 µg S/g) diets were injected s.c. with 1×10^6 control or shSep15 CT26 cells, and, after 3 weeks, mice were sacrificed and tumors were excised and weighed. B, quantitative RT-PCR analysis of Sep15 mRNA from tumor samples from mice injected with control or cells with targeted downregulation of Sep15 and mRNA from the cells. Mice were injected i.v. with 5×10^5 pU6-m3 control or shSep15 cells. Twelve days after injection, lungs were excised and bleached by Fekete's solution. C, lung metastases appear white. D, lesions formed on the surface of each lung were counted; lungs with >250 metastatic lesions were assigned a value of 250. Columns, mean (*n* = 4); bars, SE. Data are indicative of three independent experiments.

downregulation of Sep15 is protective against tumorigenesis in these colon cancer cells or that Sep15 might be important for tumorigenesis.

In contrast to these findings, previous observations have suggested that Sep15 expression is decreased in mouse liver tumors and mouse prostate adenocarcinoma cells compared with the high levels of this protein expressed by normal mouse liver and prostate (7). Similarly, Sep15 was downregulated in ~60% of human malignant mesothelioma cell lines and tumors (23). However, it should be noted that there was significant variability among the cell

lines, and 4 of the 23 mesothelioma cell lines had overexpression of Sep15. When one of the cell lines, Meso 6, was transiently transfected with small interfering RNA against *Sep15*, the cells exhibited increased cell proliferation following exposure to pharmacologic concentrations of selenium (1-25 $\mu\text{mol/L}$) compared with Meso 6 cells that possessed the wild-type *Sep15* (23). Although selenium supplementation did not influence the growth of cells with targeted downregulation of Sep15 in the current study, the cells were grown under conditions more close to the physiological state (0-1 $\mu\text{mol/L}$ Se). Moreover, differences could

Table 1. Genes and protein products whose expression was regulated by knockdown of Sep15 in CT26 colon cancer cells

Gene	Product	Fold change
Upregulated in shSep15 CT26 cells		
<i>Ccnb1ip1</i>	Cyclin B1-interacting protein 1	13.52
<i>Myoz2</i>	Myozenin 2	9.36
<i>Elovl6</i>	ELOVL family member 6, elongation of long-chain fatty acids	8.55
<i>Atp8a1</i>	ATPase, aminophospholipid transporter	7.69
<i>Tyw3</i>	TRNA-yW synthesizing protein 3 homologue	7.54
<i>Aqp1</i>	Aquaporin 1 (Colton blood group)	6.33
<i>Serpine1</i>	Serpin peptidase inhibitor, clade E	6.03
<i>Spint2</i>	Serine peptidase inhibitor, Kunitz type, 2	5.83
<i>Acadm</i>	Acyl-coenzyme A dehydrogenase	5.70
<i>Dscc1</i>	Defective in sister chromatid cohesion 1 homologue	5.52
<i>Sfmbt2</i>	Scm-like with four mbt domains 2	5.42
<i>Kcnab2</i>	Potassium voltage-gated channel, shaker-related subfamily	5.35
<i>Tuba4a</i>	Tubulin, α 4a	5.34
<i>Tcf19</i>	Transcription factor 19	5.30
<i>Chtf18</i>	CTF18, chromosome transmission fidelity factor 18 homologue	5.12
<i>Ccne2</i>	Cyclin E2	4.70
Downregulated in shSep15 CT26 cells		
<i>Lrm4cl</i>	LRRN4 COOH-terminal like	0.02
<i>Afp</i>	α -Fetoprotein	0.02
<i>Mamdc2</i>	MAM domain containing 2	0.02
<i>Dppa2</i>	Developmental pluripotency-associated 2	0.03
<i>Arhgef5</i>	Rho guanine nucleotide exchange factor 5	0.03
<i>Nefl</i>	Neurofilament, light polypeptide	0.03
<i>Avil</i>	Advillin	0.03
<i>Klf2</i>	Kruppel-like factor 2 (lung)	0.05
<i>Atp1a3</i>	ATPase, Na ⁺ /K ⁺ transporting, α 3 polypeptide	0.07
<i>Slit3</i>	Slit homologue 3 (<i>Drosophila</i>)	0.07
<i>Ifitm1</i>	IFN-induced transmembrane protein 1 (9-27)	0.08
<i>Odz4</i>	Odz, odd Oz/ten-m homologue 4 (<i>Drosophila</i>)	0.08
<i>Pla2g2e</i>	Phospholipase A2, group IIE	0.08
<i>Igfbp4</i>	Insulin-like growth factor binding protein 4	0.08
<i>Rab33a</i>	RAB33A, member RAS oncogene family	0.09
<i>Grem1</i>	Gremlin 1, cysteine knot superfamily	0.09
<i>Prss12</i>	Protease, serine, 12 (neurotrypsin, motopsin)	0.09
<i>Stard5</i>	StAR-related lipid transfer (START) domain containing 5	0.10
<i>Pdgfrb</i>	Platelet-derived growth factor receptor, β polypeptide	0.10
<i>Napb</i>	N-ethylmaleimide-sensitive factor attachment protein, β	0.11
<i>Casp4</i>	Caspase-4, apoptosis-related cysteine peptidase	0.11

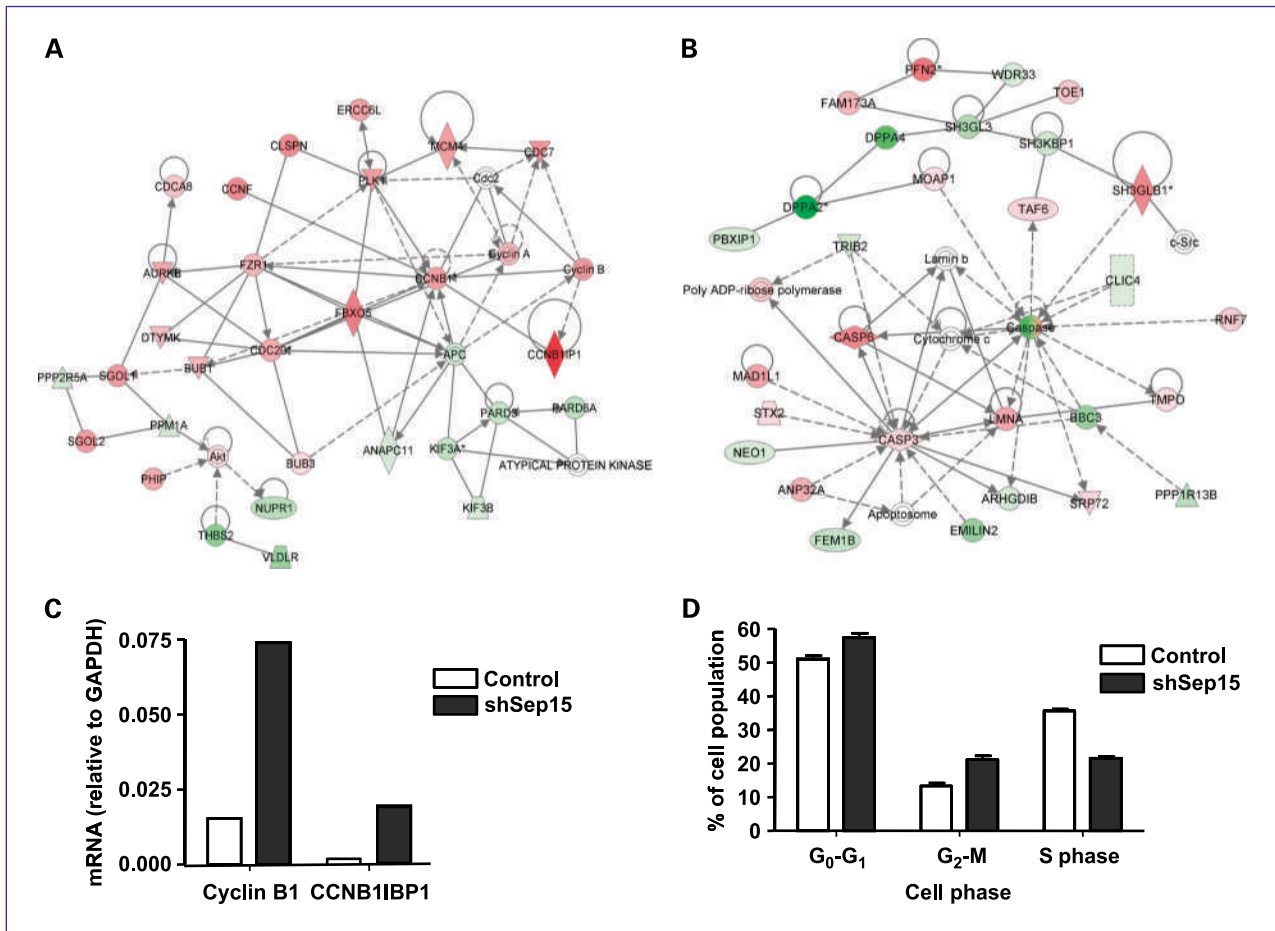


Fig. 5. Ingenuity network analysis of genes regulated by targeted downregulation of Sep15 in CT26 cells and validation by quantitative RT-PCR and cell cycle analysis. Two of the top associated networks were cell cycle/cancer (A) and cancer/cell-to-cell signaling and interaction/cellular function and maintenance (B). Probe sets identified as differentially expressed were imported into IPA software. Pink indicates an upregulation and green a downregulation of gene expression. Molecules that are not user specified, but are incorporated into the network through relationships with other molecules, are shown in white. C, quantitative RT-PCR analysis of cyclin B and CCNB1BP1 mRNA expression in control and cells with targeted downregulation. D, percent of cells in each phase of the cell cycle as determined by FACS analysis. Columns, mean ($n = 8$); bars, SE.

also be a result of transient versus stable transfection. Regardless, these data suggest that mesothelioma cells respond differently to targeted downregulation of Sep15 than CT26 colon cancer cells, suggesting that there might be tissue specificity in the response.

Apostolou et al. (23) observed that mesothelioma cells with the 1125A variant within the 3'-untranslated region of Sep15 were less responsive to the growth-inhibitory and apoptotic effects of selenium as selenocysteine than mesothelioma cells expressing the wild-type protein. It has been shown that the SECIS element with the A at position 1125 is more efficient in stimulating selenocysteine insertion than the SECIS element containing G at position 1125. Jablonska et al. (24) evaluated whether this single-nucleotide polymorphism in *Sep15* in combination with selenium status is associated with lung cancer risk. They observed that interactions between selenium status and this polymorphism in non-small cell lung cancer patients are complex and depend on the selenium status of the individ-

ual (23). Unfortunately, the expression of Sep15 in the lung tumors was not measured. However, because of the previously published data suggesting that Sep15 expression might be downregulated in certain lung cancers, as well as mouse liver and prostate tumors, we wanted to determine whether the effects might be specific to colon cancer. In contrast to observations with CT26 cells, lung carcinoma LLC1 cells transfected with the shSep15 constructs did not change growth characteristics in culture or alter their ability to grow colonies in soft agar (Fig. 3). These observations further indicate that there is tissue specificity in the response of mouse tumor cells to Sep15 status. Whereas targeted downregulation of Sep15 is protective against tumorigenesis in colon CT26 cells, it does not affect tumorigenesis in lung LLC cells. We are currently investigating whether these observations occur in human colon cancer cell lines and the mechanism(s) accounting for tissue specificity.

Although there is evidence to suggest that supplemental selenium may reduce the incidence and mortality of colon

cancer in humans (2), this effect seems to be mediated by both low molecular weight selenocompounds and selenoproteins. Moreover, not all selenoproteins may inhibit tumorigenesis. The observation that targeted downregulation of a selenoprotein may be protective against tumorigenesis is not unique for Sep15. Previous data have shown that targeted downregulation of TR1 reverses the tumor phenotype of LLC1 cells (11) and inhibits self-sufficient growth of a mouse cell line driven by oncogenic *k-ras* (DT) cells (22). TR1 is a central component in redox-regulated pathways, and its main function is to keep thioredoxin in the reduced state (25). Thioredoxin can then donate electrons to disulfides in both cytosolic and nuclear proteins and thus maintain the cysteine residues in these proteins in the reduced state. Similar to TR1, Sep15 belongs to the thiol-disulfide oxidoreductase class of selenoproteins (7, 8). Sep15 is characterized by a thioredoxin fold and has been shown to take part in the process of disulfide bond formation. Although the physiologic function and catalytic mechanism of Sep15 remain poorly understood, it has been hypothesized that Sep15 is involved in either rearrangement of disulfide bonds (isomerase function) or reduction of incorrectly formed disulfide bonds (reductase function) in misfolded glycoproteins bound to UDP-glucose:glycoprotein glucosyltransferase (8). Although it is intriguing that targeted downregulation of either TR1 or Sep15 can be protective against tumorigenesis, it is not known how these two proteins interact. Future studies are needed to investigate the interrelationship of Sep15 and TR in tumorigenesis.

Development of cancer requires multiple changes in the regulation of cell physiology. Hanahan and Weinberg (27) defined criteria that are necessary for the formation of an aggressive tumor: a cell must autonomously provide growth signals, become insensitive to growth-inhibitory signals, inactivate proapoptotic pathways, acquire a limitless replicative potential, promote angiogenesis, and become able to invade tissues and metastasize. Some tumor suppressor genes and oncogenes function specifically in these phenotypes. We used microarray technology to determine the most important genes whose expression was modified by targeted downregulation of Sep15. Although many of the changes in gene expression observed in the cells with targeted downregulation of Sep15 might be a general response to growth inhibition, microarray technology allowed us to determine the specific molecular target(s) for this growth inhibition. Interestingly, *Ccnb1ip1* was the most significantly upregulated gene in Sep15 knockdown compared with control cells (>13.5-fold increase; Table 1), which was validated by quantitative RT-PCR. This gene encodes CCNB1IP1, which functions as a RING finger family ubiquitin ligase (27).

References

1. Davis CD, Irons R. Are selenoproteins important for the cancer protective effects of selenium? *Curr Nutr Food Sci* 2005;1:201–14.
2. Clark LC, Combs GF, Jr., Turnbull BW, et al. Effects of selenium sup-

plementation for cancer prevention in patients with carcinoma of the skin. A randomized control trial Nutritional Prevention of Cancer Study Group. *JAMA* 1996;276:1957–63.

Protein ubiquitination is critical for many cellular processes through its ability to regulate protein degradation and various signaling mechanisms. CCNB1IP1 functions by modulating progression of the cell cycle through G₂-M by interacting with cyclin B and promoting its degradation (27). Alterations in the cell cycle in cells with targeted downregulation of Sep15 compared with control cells were validated by FACS analysis. CCNB1IP1 also influences the processes of cell migration and metastasis. Interestingly, human osteosarcoma cells and human breast cancer cells depleted in CCNB1IP1 both migrate more rapidly and invade more effectively than control cells (28). Similarly, downregulation of CCNB1IP1 has been associated with aggressive breast cancer and non-small cell lung cancer and predicted poor prognosis (29). Consistent with these observations, an increased expression of CCNB1IP1 was observed in the cells with targeted downregulation of Sep15, which correlated with a decreased ability to grow and metastasize.

In conclusion, the current investigations conclusively show that Sep15 shRNA transfection of mouse colon carcinoma CT26 cells (>90% reduction of Sep15 mRNA and protein levels) inhibited anchorage-dependent and anchorage-independent cell growth as well as tumor growth and lung metastasis. This response is mediated, at least in part, by increased expression of CCNB1IP1 and subsequent G₂-M cell cycle arrest in mouse colon cancer cells. Furthermore, tissue specificity in the ability of Sep15 to influence cellular proliferation was evident.

Disclosure of Potential Conflicts of Interest

No potential conflicts of interest were disclosed.

Acknowledgments

We thank Dr. John Milner (Division of Cancer Prevention, National Cancer Institute) for his helpful support, discussion, and review of the manuscript and the following individuals from the Center for Cancer Research, National Cancer Institute for their assistance: Dr. Salvador Naranjo-Suarez with the IPA analysis, Dr. Barbara Taylor with FACS analysis, and Dr. Paul Goldsmith with the catalytic assays.

Grant Support

National Cancer Institute Intramural support; Cancer Prevention Fellowship Program; Division of Cancer Prevention, National Cancer Institute; and NIH grant CA080946.

The costs of publication of this article were defrayed in part by the payment of page charges. This article must therefore be hereby marked *advertisement* in accordance with 18 U.S.C. Section 1734 solely to indicate this fact.

Received 01/11/2010; revised 02/18/2010; accepted 02/23/2010; published OnlineFirst 04/13/2010.

3. Davis CD, Uthus EO. Dietary folate and selenium affect dimethylhydrazine-induced aberrant crypt formation, global DNA methylation and one-carbon metabolism in rats. *J Nutr* 2003;133:2907–14.
4. Jao SW, Shen KL, Lee W, Ho YS. Effect of selenium on 1,2-dimethylhydrazine-induced intestinal cancer in rats. *Dis Colon Rectum* 1996;39:628–31.
5. Irons R, Carlson BA, Hatfield DL, Davis CD. Both selenoproteins and low molecular weight selenocompounds reduce colon cancer risk in mice with genetically impaired selenoprotein expression. *J Nutr* 2006;135:1311–7.
6. Kryukov GV, Castellano S, Novoselov SV, et al. Characterization of mammalian selenoproteomes. *Science* 2003;300:1439–43.
7. Kumaraswamy E, Malykjh A, Korotkov KV, et al. Structure-expression relationships of the 15-kDa selenoprotein gene. *J Biol Chem* 2000;275:35540–7.
8. Labunskyy VM, Hatfield DL, Gladyshev VN. The Sep15 protein family: roles in disulfide bond formation and quality control in the endoplasmic reticulum. *IUBMB Life* 2007;59:1–5.
9. Nasr MA, Hu YJ, Diamond AM. Allelic loss of the Sep15 locus in breast cancer. *Cancer Ther* 2004;1:293–8.
10. Corbett TH, Griswold DP, Jr., Roberts BJ, Peckham JC, Schabel FM, Jr. A mouse colon-tumor model for experimental therapy. *Cancer Chemother Rep* 1975;5:169–86.
11. Yoo MH, Xu XM, Carlson BA, Gladyshev VN, Hatfield DL. Thioredoxin reductase 1 deficiency reverses tumor phenotypes and tumorigenicity of lung carcinoma cells. *J Biol Chem* 2006;281:13005–8.
12. Xu XM, Mix H, Carlson BA, et al. Evidence for direct roles of two additional factors, SECp43 and soluble liver antigen, in the selenoprotein synthesis machinery. *J Biol Chem* 2005;280:41568–75.
13. Carlson BA, Xu XM, Gladyshev VN, Hatfield DL. Selective rescue of selenoprotein expression in mice lacking a highly specialized methyl group in selenocystein tRNA. *J Biol Chem* 2005;280:5542–8.
14. Paglia DE, Valentine WN. Studies on the quantitative and qualitative characterization of erythrocyte glutathione peroxidase. *J Lab Clin Med* 1967;70:158–69.
15. Holmgren A, Björnstedt M. Thioredoxin and thioredoxin reductase. *Methods Enzymol* 1995;252:199–208.
16. Hill KE, McCollum GW, Burk RF. Determination of thioredoxin reductase activity in rat liver supernatant. *Anal Biochem* 1997;253:123–5.
17. Hintze KJ, Wald KA, Zeng H, Jeffery EH, Finley JW. Thioredoxin reductase in human hepatoma cells is transcriptionally regulated by sulforaphane and other electrophiles via an antioxidant response element. *J Nutr* 2003;133:2721–7.
18. Huang DW, Sherman BT, Lempicki RA. Systematic and integrative analysis of large gene lists using DAVID bioinformatics resources. *Nat Protoc* 2009;4:44–57.
19. Dennis G, Jr., Sherman BT, Hosack DA, et al. DAVID: Database for Annotation, Visualization, and Integrated Discovery. *Genome Biol* 2003;4:P3.
20. Xu XM, Yoo MH, Carlson BA, Gladyshev VN, Hatfield DL. Simultaneous knockdown of the expression of two genes using multiple shRNAs and subsequent knock-in of their expression. *Nat Protoc* 2009;4:1338–48.
21. Yoo MH, Xu XM, Turanov AA, Carlson BA, Gladyshev VN, Hatfield DL. A new strategy for assessing selenoprotein function: siRNA knock-down/knock-in targeting the 3'-UTR. *RNA* 2007;3:921–9.
22. Yoo MH, Xu YM, Carlson BA, Patterson AD, Gladyshev VN, Hatfield DL. Targeting thioredoxin reductase 1 reduction in cancer cells inhibits self-sufficient growth and DNA replication. *PLoS One* 2007;2:e1112.
23. Apostolou S, Klein JO, Missuuchi Y, et al. Growth inhibition and induction of apoptosis in mesothelioma cells by selenium and dependence on selenoprotein *SEP15* genotype. *Oncogene* 2004;23:5032–40.
24. Jablonska E, Gromadzinska J, Sobala W, Reszka E, Wasowicz W. Lung cancer risk associated with selenium status is modified in smoking individuals by *Sep15* polymorphism. *Eur J Cancer* 2008;47:47–54.
25. Arner ES, Holmgren A. Physiological functions of thioredoxin and thioredoxin reductase. *Eur J Biochem* 2000;267:6102–9.
26. Hanahan D, Weinberg RA. The hallmarks of cancer. *Cell* 2000;100:50–70.
27. Toby GG, Gherraby W, Coleman TR, Golemis EA. A novel RING finger protein, human enhancer of invasion 10, alters mitotic progression through regulation of cyclin B levels. *Mol Cell Biol* 2003;23:2109–22.
28. Singh MK, Nicolas E, Gherraby W, Dadke D, Lessin S, Golemis EA. He110 negatively regulates cell invasion by inhibiting cyclin B/cdk1 and other promotility proteins. *Oncogene* 2007;26:4825–32.
29. Confalonieri S, Quarto M, Goisis G, et al. Alteration of ubiquitin ligases in human cancer and their association with the natural history of the tumor. *Oncogene* 2009;28:2959–68.